Fig. 1: Microtubule assembly using N- and C-terminally double truncated tau type IA and type IB molecules.

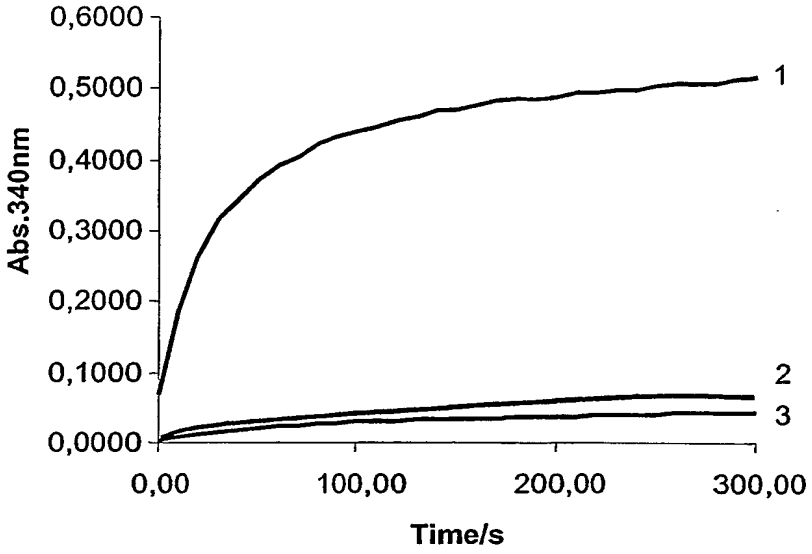

Microtubule assembly using normal healthy tau (1), tau type IA (2) and tau type IB (3).

Fig. 2: Inhibition of microtubule assembly using N- and C-terminally double truncated tau type IA and type IB molecules.

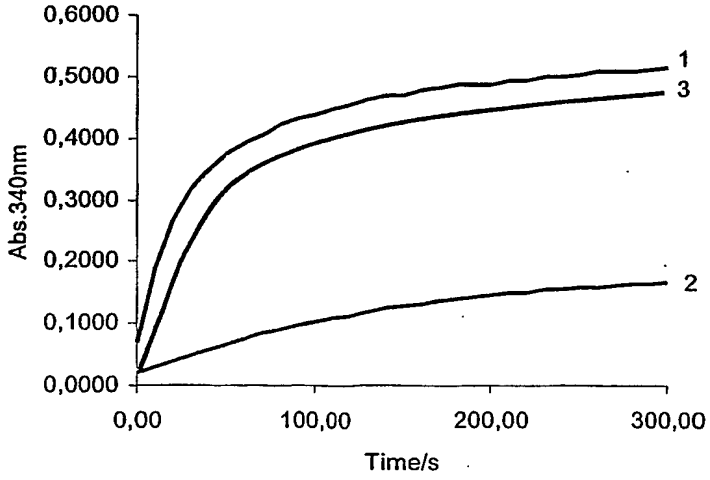

Microtubule assembly using (1) healthy *tau*, (2) inhibition by tau type IA, (3) lack of inhibition when using *tau* type IB.

Fig. 3: Activity of N- and C-terminally double truncated tau type IIA and IIB molecules in microtubule assembly.

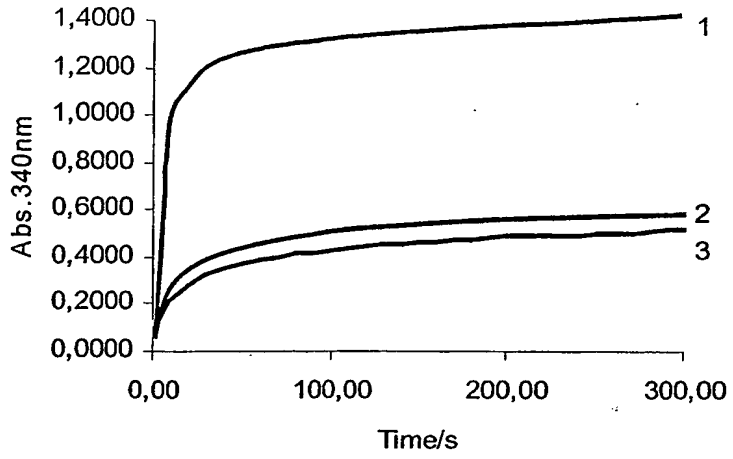

Strong promotion of microtubule assembly in the presence of recombinant tau type IIA (1). Microtubule assembly using normal healthy tau (2) and with recombinant *tau* type IIB (3)

Fig. 4: Type IIA N- and C- terminaly double truncated tau expressed in neuronal cells significantly increases their sensitivity to oxidative stress.

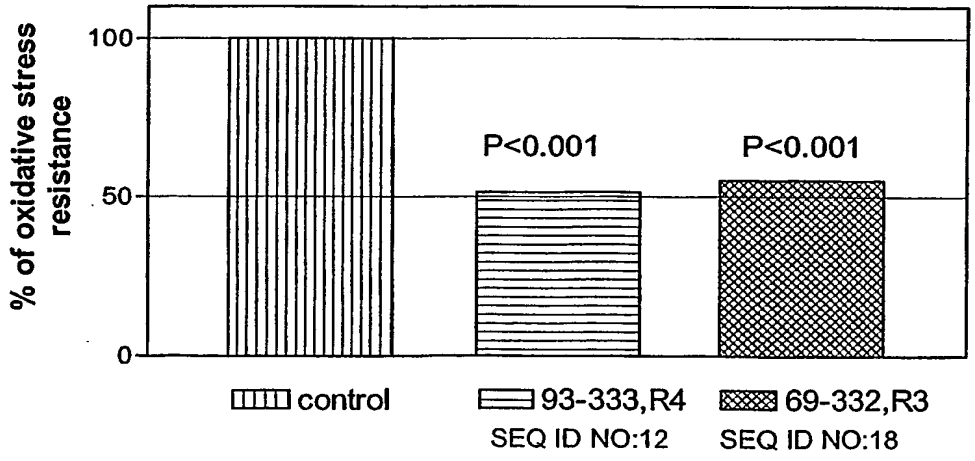

The bar chart represents the decrease in relative resistance to oxidative stress of neuronal cells with the presence of tau type IIA. Resistance of cells non-harboring the said protein (control) is expressed as 100% (left bar) and resistance of neuronal cells expressing the diseased tau protein are shown as % of the control value (middle and right bar). Resistance is defined as the concentration of free radicals generated by SIN-1 in culture medium, where 50% of the cells die. The results represent measurement of double truncated tau proteins type IIA SEQ ID NO:12 (93-333, R4) and SEQ ID NO:18 (69-332, R3), respectively.

Fig. 5: Affinity of a monoclonal antibody to diseased tau type IA protein and its deletion mutants.

Deletion mutant	Epitope deleted	Apparent affinity [nM]
SEQ ID NO 1 (239-333, R4)	-	10
SEQ ID NO 22 (248-333, R4; del 239-247)	A1	20
SEQ ID NO 23 (258-333, R4; del 239-257)	A2	40
SEQ ID NO 24 (263-333, R4; del 239-262)	A3	200
SEQ ID NO 25 (239-333, R4; del 248-262)	A4	100
SEQ ID NO 26 (239-333, R4; del 256-262)	A5	40
SEQ ID NO 27 (239-333, R4; del 263-267)	A6	300
SEQ ID NO 21 (268 -333, R4; del 239-267)	A	10000

Fig. 6: Fractionation of *tau* derived from AD-brain extracts using Superdex 200-columns.

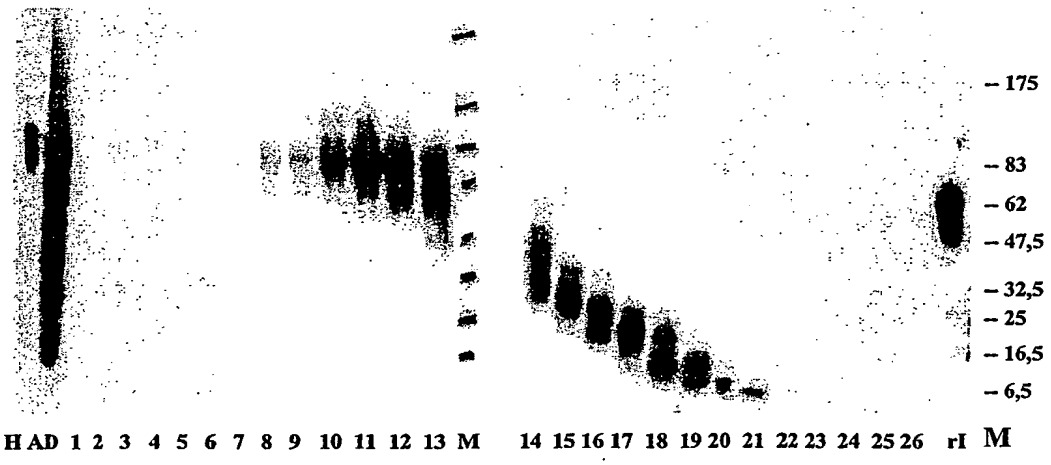

H: *Tau* from healthy brain before fractionation, AD: *Tau* from AD brain before fractionation, 1-26: individual fractions, rI: six isoforms of *tau* (recombinant, pooled), M: molecular weight markers.

Fig. 7: Detection of *tau* type IA inhibitory activity in three separate isolations of fraction 19.

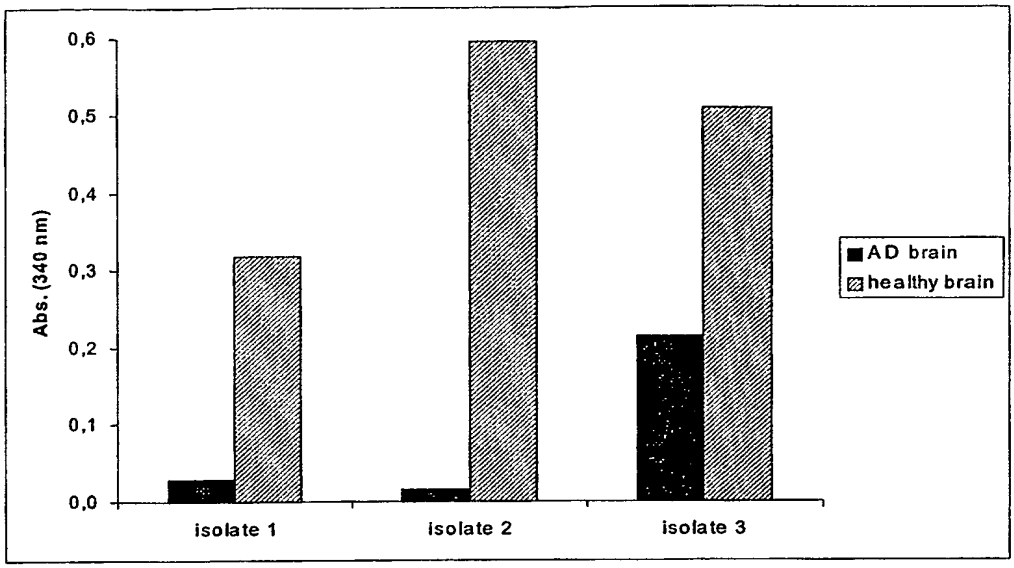

Tau preparations from fraction 19 of AD and healthy brains were mixed with normal healthy *tau*, tubulin and GTP at 4°C. The samples were loaded into preheated cuvettes (37°C) and the changes in turbidity after 5 min. was measured using a temperature controlled spectrophotometer.

Fig. 8: Occurence of N- and C- terminally truncated *tau* molecules in AD brain.

Demonstration of N- and C-terminally double truncated tau type I

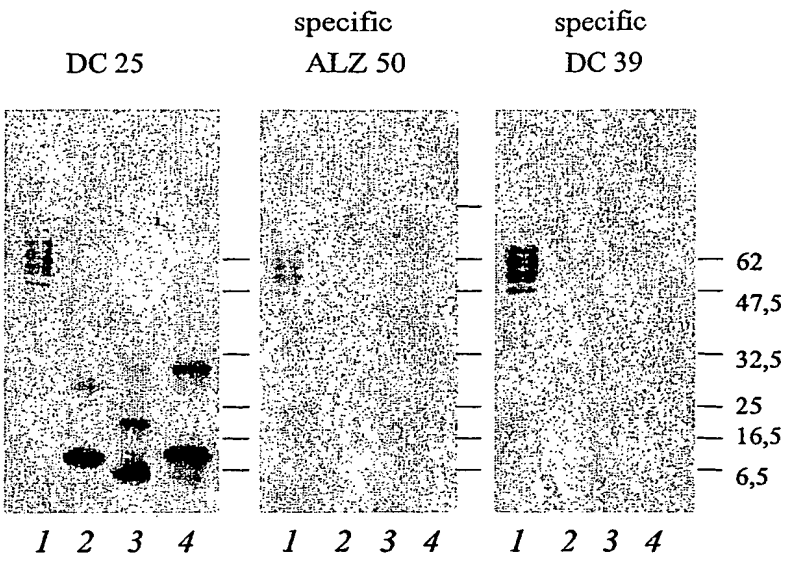

Western blot analysis of using mABs DC25, ALZ50 and DC39.
Lane 1: Recombinant six isoforms of human *tau*. Lanes 2-4: Three different preparations of fraction 19 from AD brain.

Fig. 9: Western blot using antibody DC25: Detection of *tau* type I in AD brain but not in healthy brain.

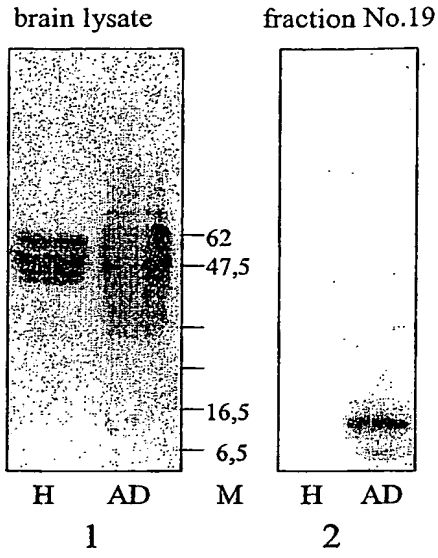

Tau type I proteins are present in Alzheimer brain lysates (AD) and absent in normal healthy brain (H) as demonstrated by Western blot. M: molecular weight marker. Proteins resolved by SDS-PAGE were transfered to PVDF membranes and probed with antibody DC25.

1. Extracts from healthy brain (H) and Alzheimer's disease brain (AD).

2. Fraction No. 19 from healthy brain (H, does not contain type IA molecules) and Alzheimer's disease brain (AD) extracts after gel chromatography on Superdex 200 column.

Fig 10: Immunoreactivity of N- and C- terminally double truncated tau type II molecules.

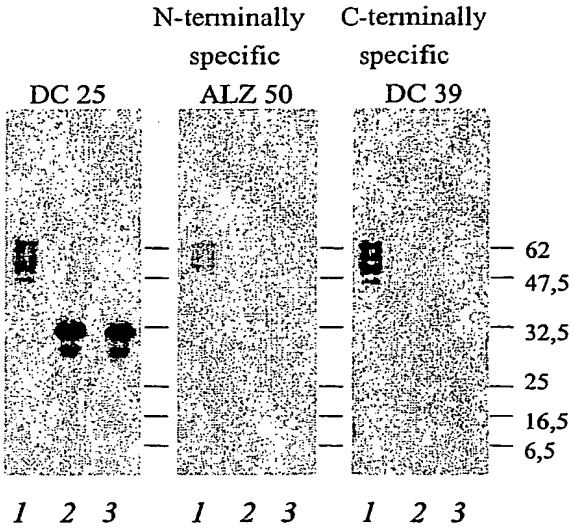

Proteins resolved by SDS PAGE (5-20% acrylamide) were transfered to PVDF membranes. Blots were probed with three different mAbs: DC25, ALZ50 and DC39.

Lanes:
1.Recombinant six isoforms of human tau.
2-3. Two different preparations of fraction #15 from AD-brains.

Fig. 11:

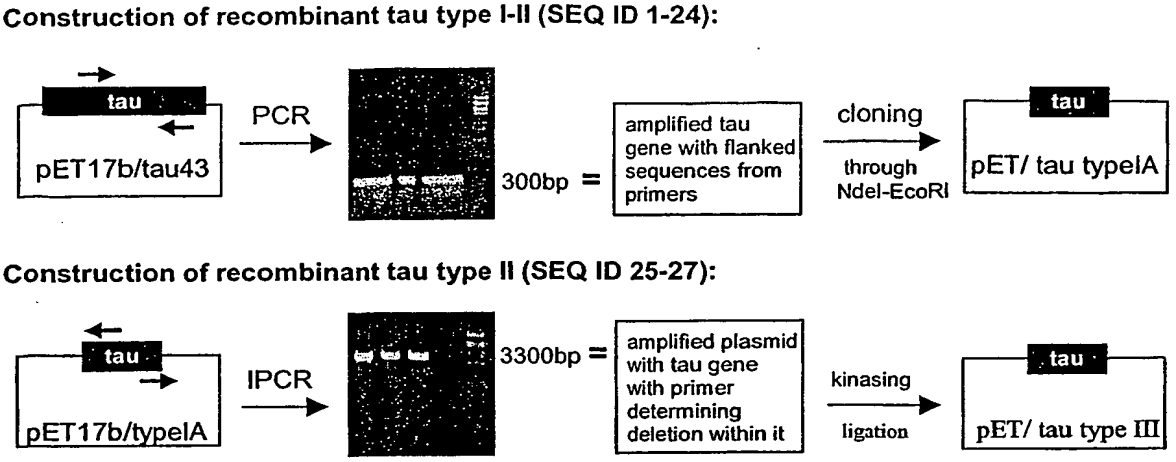

Fig. 12: Inhibitory effect in microtubule assembly of brain derived or recombinant *tau* type IA.

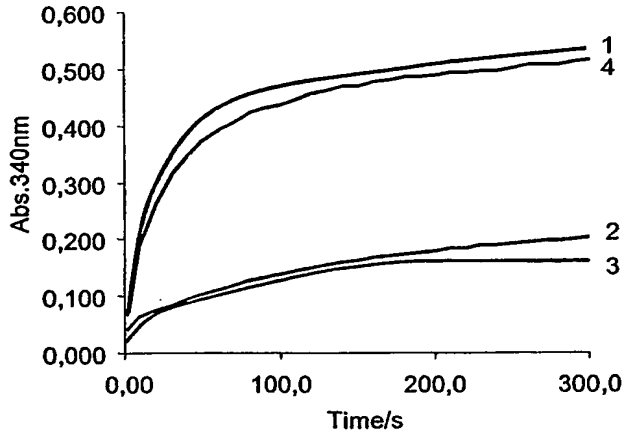

Fig. 13: First round screening of drug candidates neutralizing tau type IA molecules (step 1)

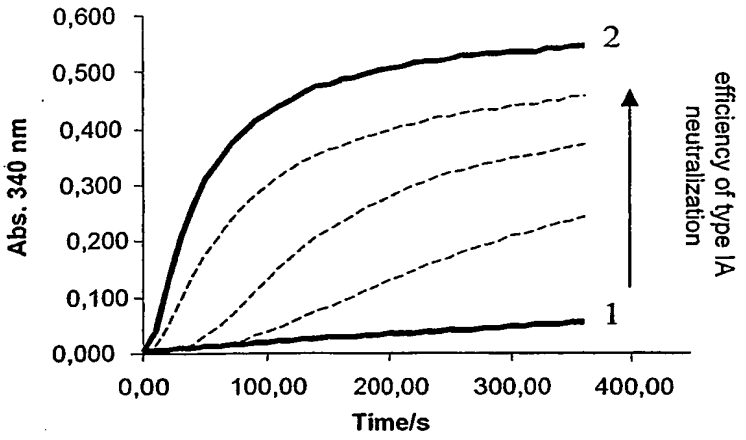

A drug candidate was preincubated with type IA molecule and efficiency of type IA neutralization was assayed in microtubule assembly. Bottom curve 1 and top curve 2 represent negative (no neutralization) and positive (100%) neutralizing activity of tested drug candidate against diseased type IA molecules. Middle curves indicate various efficiencies of type IA-neutralization by three different drug candidates.

Fig. 14: Second round screening for drug candidates neutralizing type IA molecules with selectivity against normal *tau* (step 2).

Selection of drug candidates not inhibiting healthy tau

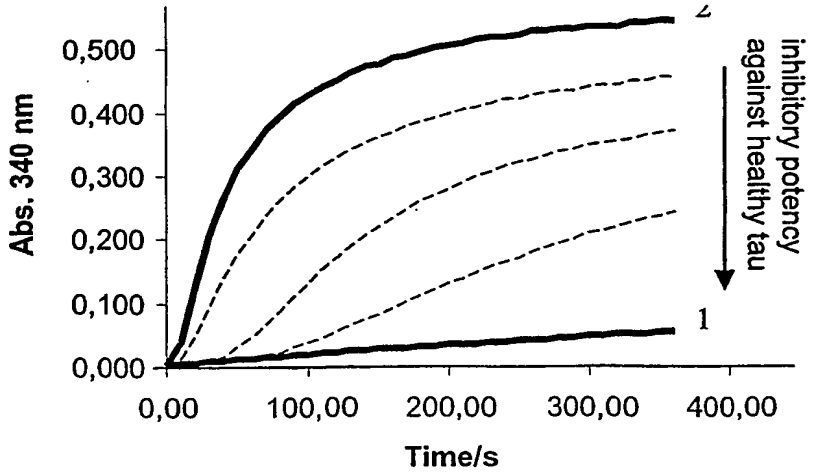

Drug candidates selected in step 1 were preincubated with healthy tau and the effect on microtubule assembly was assayed. The bottom curve (1) shows inactivation of healthy tau thus no selectivity. The top curve (2) shows no inhibition of healthy *tau*, thus high specificity for the diseased forms. The middle curves show drug candidates with various levels of specificity against healthy *tau*.

Fig. 15: First round screening for drug candidates neutralizing tau type IIA.

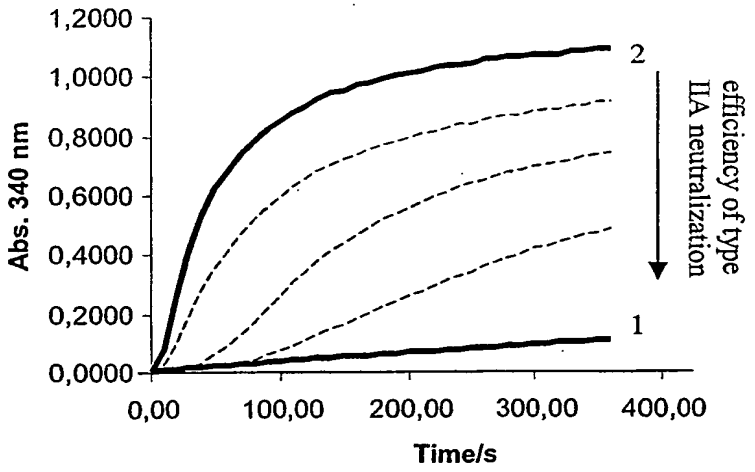

Drug candidate was preincubated with type IIA molecule and efficiency of type IIA neutralization was assayed in microtubule assembly. Bottom curve 1 represents positive (100%) neutralizing activity of respective drug candidate and top curve 2 indicates no neutralization of diseased type IIA molecules. Middle curves indicate different efficiency of various drug candidates in type IIA-neutralization.

Fig. 16: Second round screening for drug candidates capable to neutralize tau type IIA molecules and discriminate them from normal tau (step 2).

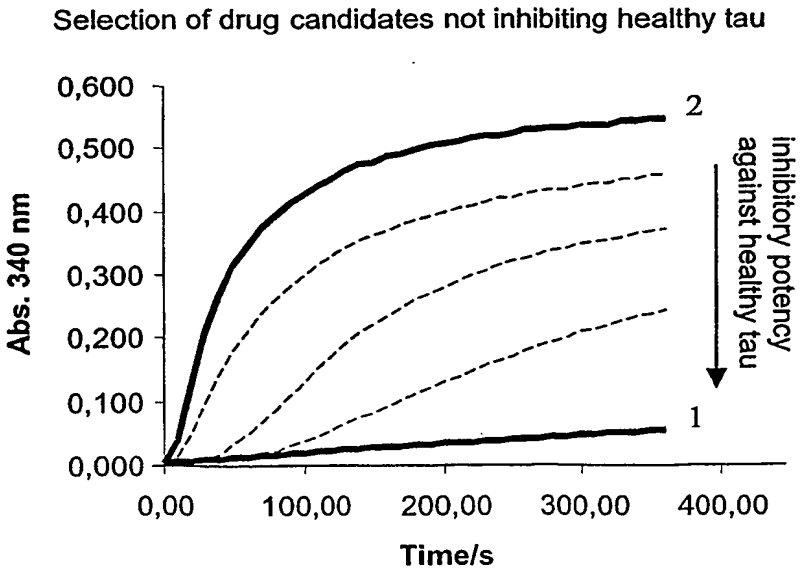

Drug candidates selected in step 1 were preincubated with healthy tau and the effect on microtubule assembly was assayed. The bottom curve (1) represents maximal inhibition of healthy tau and the top curve (2) indicates no inhibition of healthy tau. Middle curves show drug candidates with different inhibitory activity against healthy tau.

Fig. 17: Specific antibody levels in prefused mice sera determined by ELISA

The levels of specific antibodies in sera of mice immunized with AD derived tau were tested in ELISA on the same antigen. All five sera showed high anti-tau binding activity to said tau protein. Figure 17 represents levels of specific antibodies in one of the immunized mice. As a control was used serum from the mouse immunized with irrelevant protein.

Fig. 18: ELISA reactivity of monoclonal antibodies with AD-brain derived tau (fraction #19) and control healthy brain-derived *tau*.

Mabs	ELISA(A492nm) AD – *tau*	healthy *tau*	Immunogen	Epitope	Isotype
DC44#	1,42	0,31	AD(Fr.#19)*	aa300-317	IgM/κ
DC82	1,81	0,12	AD(Fr.#19)*	aa300-317	IgG2b/κ
DC136	1,52	0,18	AD(Fr.#19)*	aa300-317	IgG2a/κ
DC25	1,91	1,81	tau43	aa347-353	IgG1/κ
DC20	0,18	0,12	IFNα	ND	IgG1/κ

#DC44:deposited on 4 June 2002 at the ECACC Porton Down, Salisbury, Wilts, UK under the deposition number 02060767; * the immunogen for these antibodies was N-and C-terminally truncated tau type I proteins isolated from Alzheimer brains (fraction 19); DC 20: monoclonal antibody with irrelevant specificity. Shown data represent mean values from three parall experiments.

Fig. 19. ELISA reactivity of monoclonal antibodies with recombinant tau molecules.

ELISA (A492 nm)

	Recombinant forms of tau molecules		
	Double truncated proteins		Full length
Mabs	TypeIA (SEQIDNO:1)	TypeIIA (SEQIDNO:12)	six isoforms
DC44	1,72	1,61	0,21
DC82	1,51	1,52	0,17
DC136	1,59	1,78	0,13
DC25	1,71	1,51	1,98
DC20	0,11	0,07	0,09

DC 20: monoclonal antibody with irrelevant specificity
Shown data represent mean values from three paralles

Fig. 20: Screening for neutralizing antibodies directed against AD-brain derived tau type IA (fraction #19).

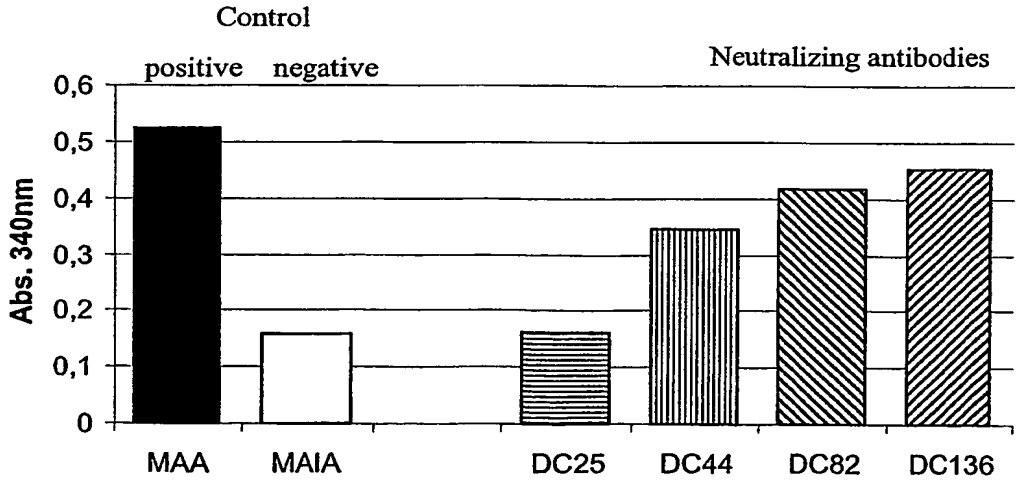

Antibodies were preincubated with native tau type IA (fraction #19) and subsequently mixed with healthy human *tau*, tubulin and GTP. The formation of microtubules was determined spectrophotometrically after 5 min at 37^{0}C. The bars represent a mean value of three independent experiments. MAA – microtubule assembly assay with healthy human tau. MAIA – microtubule assembly inhibition assay with healthy human tau preincubated with tau type IA (without antibody).

Fig. 21: Screening for neutralizing antibodies directed against recombinant *tau* type IA (SEQ ID NO:1).

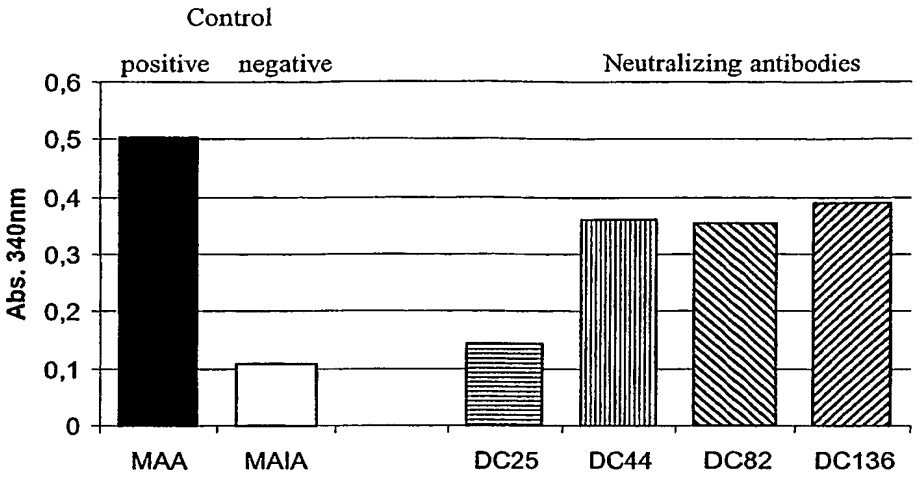

Fig. 22: Screening for drug candidates capable of neutralizing *tau* type IA molecules and of discriminating them from healthy *tau*.

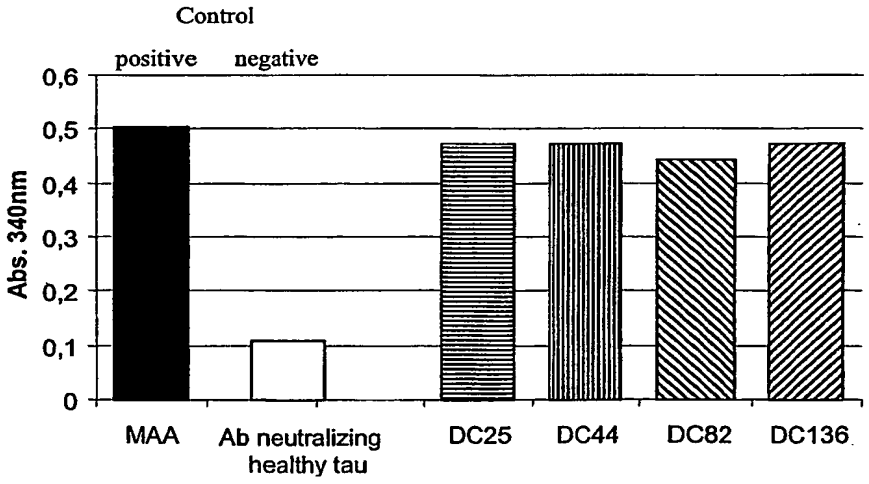

Antibodies neutralizing tau type IA were preincubated with healthy tau and subsequently mixed with tubulin and GTP. The formation of microtubules was determined spectrophotometrically after 5 min at 37^{0}C. The bars show the mean value of three independent experiments. MAA – microtubule assembly assay with healthy tau. As a negative control an antibody neutralizing healthy tau was used.

Fig 23: Neutralization of pathological activity of recombinant tau type IIA (SEQ ID NO: 12) by monoclonal antibodies

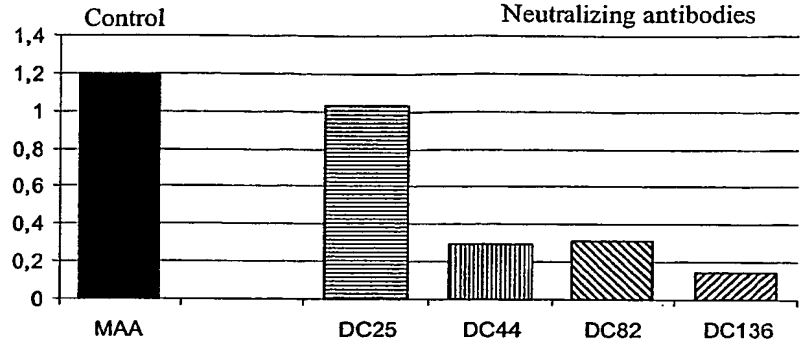

Antibodies were preincubated with recombinant tau type IIA and then mixed with tubulin and GTP. The formation of microtubules was determined spectrophotometrically after 5 min at 37°C. The bars represent the mean value of three independent experiments. MAA – microtubule assembly assay with tau type IIA (without antibody).

Fig 24: Levels of antibodies against recombinant tau type IIA (SEQ ID NO.:12) detected by ELISA.

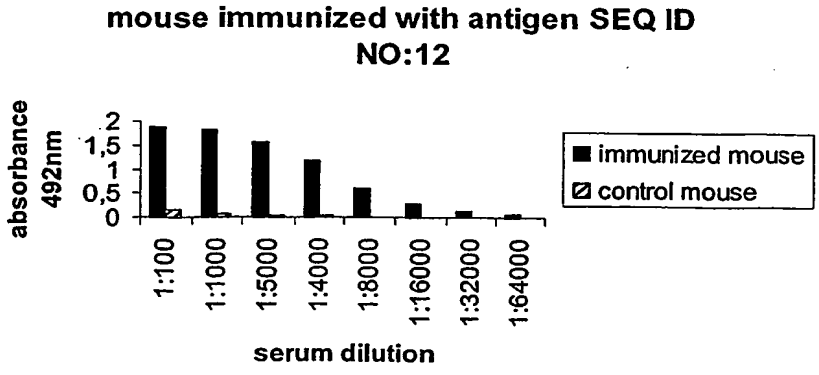

Fig 25: Genotyping of transgenic animals.

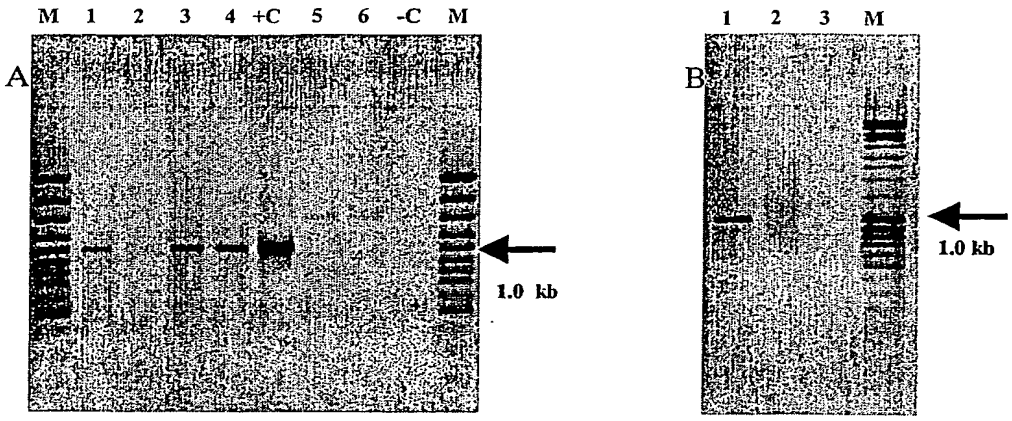

Panel A shows genotyping of the parental generation of transgenic animals. Specific amplification of double truncated sequence of DNA from genomic DNA in lanes 1, 2, 3 and 4 indicates the presence of a specific transgene in genomic DNA extracted from tails of the progeny of foster mothers. These animals represent the parental generation of transgenic animals bearing double truncated type IIA *tau* molecules. In this example, positive (+C) and negative (-C) and two additional negative samples (5, 6) are shown (M=size marker). The arrow indicates the expected PCR product size expected in transgene positive animals.
Panel B. Genotyping of animals from F1 generation. Genomic DNA was extracted from tail tips and double truncated tau specific DNA sequence was identified and are shown in lanes 1. Lane 2 and 3 show negative controls. Identification of a *tau* specific DNA fragment in the F1 generation confirms the inheritability of these transgenes.

Fig. 26: Gene expression of double trucated human *tau* transcripts in the F1 generation of transgenic animals.

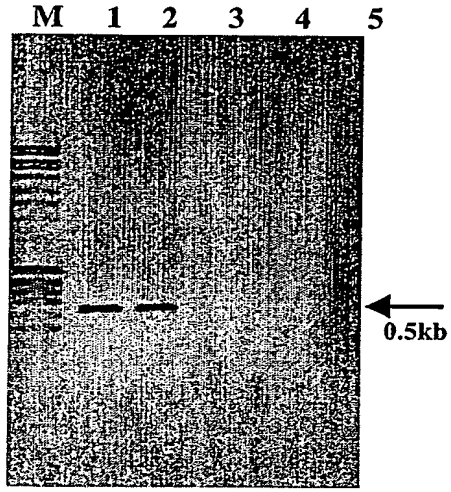

RNA was extracted from flash frozen tissue of transgenic animals and subjected to reverse transcription followed by specific amplification of the cDNA. An example shows transgene expressing animals in lanes number 1 and 2. Lanes 3-5 represent non-expressing controls while lane 5 shows a non-specific signal typically emerging in non-transgenic animal when using this method. This example indicates the presence of double truncated *tau* specific mRNA experssed from the transgene in experimental animals.

Fig. 27: Cell death caused by type IIA molecule overexpression after 6 day *in vitro* differentiation.

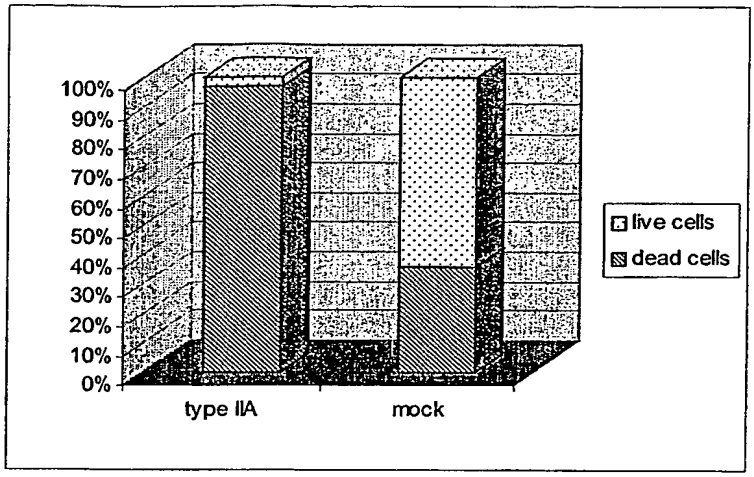

Comparison of the cell viability of SY5Y cells transfected with double truncated *tau* type IIA (type IIA) and non-transfected control neuron-like cells (mock), respectively.

Fig. 28A: Increased binding affinity of type IIA molecules to microtubules.

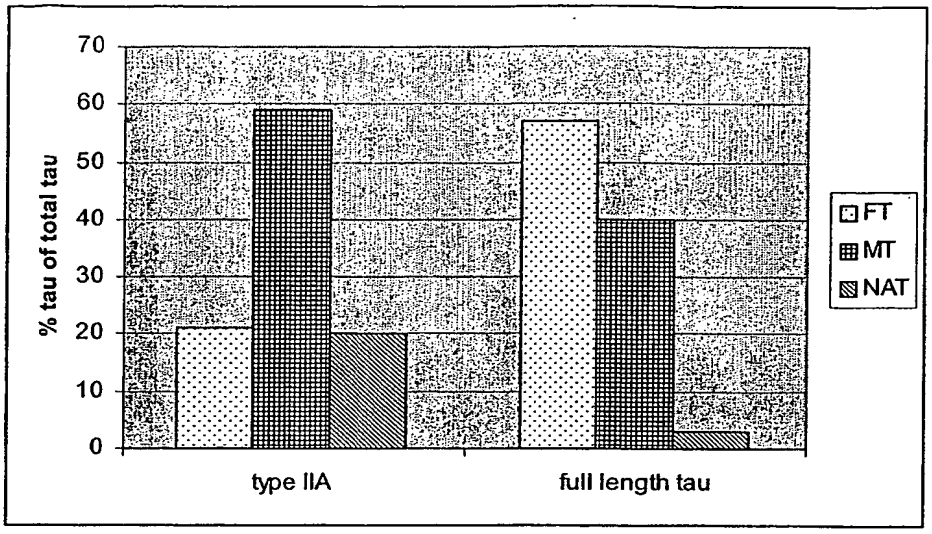

Increased binding affinity of type IIA molecules to microtubules is demonstrated by using cellular fractionation of stably transfected cells expressing type IIA double truncated molecules and full-length *tau*. Isolation of free *tau* (FT), microtubule bound *tau* (MT) and nucleus associated *tau* (NAT) was performed as described.

Fig. 28B: Inhibition of tau type IA or type IIA microtubule polymerisation by F123.

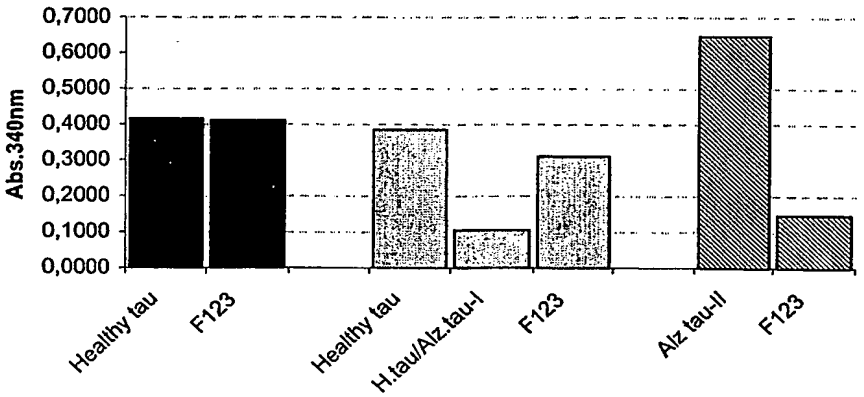

Fig. 28C: Micotubule Assembly: comparison between Seq.ID No 10 and tau 43

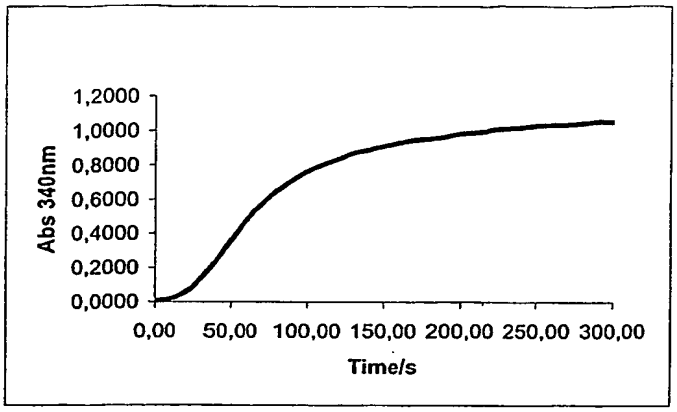

Mikrotubuli-assembly – (Seq. ID 10 und 12)
end concentration 100ug/ml; tubulin:

Elektron microscopic analysis of assembled microtubuli in the presence of tau Type IIA (Beispiel - Seq. ID 12). magnification 2600x.

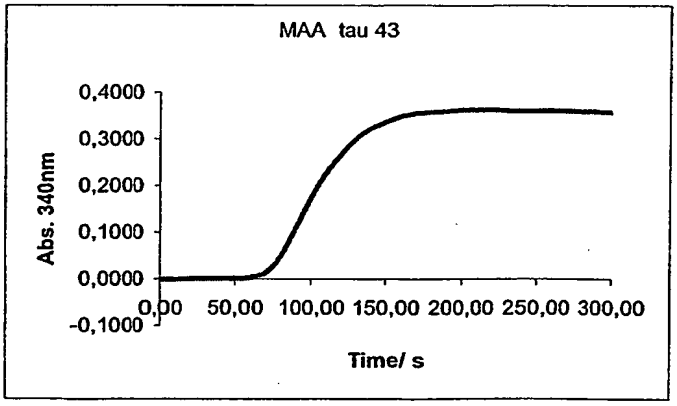

Tau: recombinant isoform Tau 43; end concentration 200ug/ml
Tubulin: end concentration 2mg/ml

Elektron microscopic analysis of assembled microtubuli in the presence of recombinant tau 43. magnification 2600x.

Fig. 29: Logarithmically growing SH-SY5Y cells stained with MitoFluor. Regular distribution of mitochondria in cell bodies and processes.

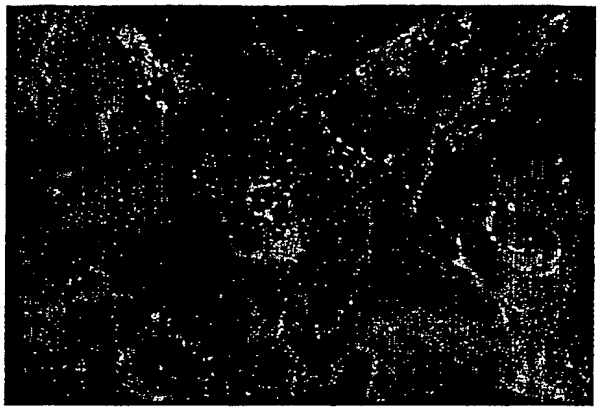

Fig. 30: Logarithmically growing *tau* type IIA expressing SH-SY5Y cells stained with MitoFluor. Perinuclear clustering of green-labelled mitochondria around the centrosome area of the cell.